Electron Injection and Recombination in Fluorescein 27−Sensitized TiO 2 Thin Films

ARTICLE *in* THE JOURNAL OF PHYSICAL CHEMISTRY B · FEBRUARY 2001

Impact Factor: 3.3 · DOI: 10.1021/jp002010s

Electron Injection and Recombination in Fluorescein 27-Sensitized TiO_2 Thin Films

Gábor Benkö,[†] Marcus Hilgendorff,[‡] Arkady P. Yartsev,[†] and Villy Sundström*[,†]

Department of Chemical Physics, Lund University, P.O. Box 124, S-22100 Lund, Sweden, and Hahn-Meitner Institute, Glienickerstrasse 100, D-14109 Berlin, Germany

Received: June 2, 2000; In Final Form: October 23, 2000

Electron injection and recombination dynamics of the dye Fluorescein 27 adsorbed to a nanocrystalline titanium dioxide (TiO_2) thin film in acetonitrile (CH_3CN) were studied by femtosecond pump−probe spectroscopy. After excitation of the dye at the absorption maximum, transient absorption spectra and kinetics were recorded in the spectral region between 400 and 2000 nm. It was found that most of the transient spectrum is dominated at early times by induced excited-state absorption (ESA). Even in the near-IR spectral region, where the ESA of the dye in aqueous solution is less than the noise level of our measurements, a pronounced ESA of the dye/TiO_2 system has been observed. Photoproduct formation following electron injection from the dye molecule into the conduction band of the semiconductor can be resolved in spectral regions where ESA is either canceled by stimulated emission (SE) or is compensated by ground-state absorption bleach at early times. The remaining signals at these wavelengths reflect the dynamics of photoproducts, which are conduction-band electrons in TiO_2 and oxidized Fluorescein 27 dye molecules. The kinetics of SE decay and the rise times of induced absorption of photoproducts are ultrafast and nonexponential, requiring at least three time constants ranging from <100 fs to ∼8 ps. The depopulation of the excited state monitored by SE decay corresponds very well to the formation of the photoproducts. Recombination is also nonexponential, part of it happens in tens of picoseconds, but the major part does not occur on the investigated time scale (until 500 ps). The possibility of resolving the dynamics of both precursor and product species in Fluorescein 27−TiO_2 nanoparticle thin films makes it suitable for spectroscopicaly studying interfacial electron transfer as a function of system parameters.

I. Introduction

Sensitization of wide band gap semiconductors to visible light consists in adsorption of molecular dyes to a semiconductor surface. Light-induced electron transfer in such dye-sensitized semiconductors (e.g., ZnO, SnO_2, and TiO_2) is not only important from a fundamental standpoint but also has significant practical importance. A wide range of applications has been considered such as photography,[1,2] electrophotography,[3] fuel-producing photochemical redox reactions,[4,5] photogalvanic cells,[5] detoxification and purification processes,[6] and photoelectrochemical cells. Considerable technological interest has recently appeared for application of semiconductor materials in solar cells, as light-to-electricity conversion efficiencies are now approaching commercially viable levels.[7−9] The lower sensitivity of the photovoltage-to-light intensity variations in solar cells based on dye-sensitized semiconductors, as compared to conventional silicon devices**,** is another attractive property of these cells. The photoelectrochemical device developed by Grätzel and co-workers[9] employs a thin (∼10 μm) nanocrystalline TiO_2 film attached to a SnO_2 conducting glass support and is covered by a Ru−bipyridyl-based sensitizer. The nanostructured, porous (typically a porosity of 50−60% is achieved) film provides the highest possible surface-to-volume ratio for sensitization. A simplified picture of energy conversion from light to electricity in these solar cells involves the following steps: excitation of dye molecules with visible light leads to electron injection from the excited state of the dye into the semiconductor film. Injected electrons migrate through the interconnected spongelike network of semiconductor particles and are collected by the conducting electrode. The dye becomes oxidized and must therefore be regenerated by a redox system, an electrolyte solution containing I^-/I_3^- ions which penetrate into the structure of the film and is sandwiched by another conducting glass covered with platinum. The oxidized dye molecules are reduced by I^- ions, regenerating the original dye molecules. The oxidized iodine diffuses to the back electrode as I_3^- ions, where reduction occurs to sustain a cyclic process. The critical processes for energy conversion are electron injection and the two possible recombination pathways, occurring at the interface: injected electrons may recombine either with oxidized dye molecules or with redox species. For an efficient light-to-current conversion process it is necessary to establish conditions in the sensitized film for fast electron injection combined with much slower recombination, to allow time for complete reduction of the oxidized dye through the redox system.

In recent years, electron transfer between TiO_2 nanoparticles and dye sensitizers has been intensely studied by transient optical spectroscopy. The rates of electron injection for different dyes were reported to be in the femtosecond time domain.[10−22] Rates for recombination were reported to range from tens of picoseconds up to milliseconds.[10−25] However, the nature of the processes and the parameters controlling the rates of electron injection and recombination are not yet well established. A

* Corresponding author. Fax: +46 46 2224119. E-mail: Villy.Sundstrom@chemphys.lu.se.
[†] Lund University.
[‡] Hahn-Meitner Institute.

10.1021/jp002010s CCC: $20.00
Published on Web 01/17/2001

detailed understanding of the reaction mechanisms would allow fine-tuning optimization of these systems.

In many of the studies, the rate of electron injection was obtained by measuring transient absorption excited-state dynamics of the dye or of the photoproducts arising from the oxidized dye, or by measuring the fluorescence decay (or equivalently the SE decay) of the dye/semiconductor system. The major challenge of all transient absorption studies carried out in the visible and near-IR spectral regions is the strong spectral overlap of the various transient species. ESA, cationic-state(s) absorption, SE, ground-state bleach of the sensitizer, and absorption of injected electrons all occur in this part of the electromagnetic spectrum. As a consequence, reports on electron transfer in these systems have sometimes been conflicting[11,17] and subject to debates.[12,18]

Studies carried out in the mid-IR spectral region proposed a new trend in the direct study of electron transfer at solid−liquid interfaces. It was suggested by Lian et al.[13−16] that IR-probing (4−6 μm) avoids the difficulties in the visible and near-IR spectral regions and monitors the arrival of electrons in the conduction band of the TiO_2. From the rise time of the infrared signal in the study of $Ru(dcbpy)_2(NCS)_2/TiO_2$ film it was concluded that the major part of the injection occurs in 50 ± 25 fs. In a recent study, Klug et al.[19] reported electron injection and recombination, using visible wavelengths for probing, with both ruthenium bipyridyl [$Ru(dcbpy)_2(NCS)_2$] and porphyrin sensitizer dyes. For the ruthenium dye, the electron injection kinetics were obtained from the appearance of dye cation absorption at 760 nm; for the two porphyrin dyes, the electron injection kinetics were obtained from the decay of a SE band. Remarkably, these authors observe almost indistinguishable nonexponential kinetics for all three dyes. The observed very fast (<100 fs) component is similar to the mid-IR data,[15] but the overall injection process appears to be much slower from the visible probing[19] because of significant contributions of slower components (~1 ps, and ~10 ps). As debated in the literature, kinetics probed in the near-IR[19] might be affected by the complicated photoinduced spectral dynamics, as well as by an interaction between photoexcited molecules.

The apparent difference in electron injection dynamics depending on the choice of probe spectral region naturally raises the question of which technique best captures the electron dynamics. Alternatively, could it be that various methods are sensitive to different parts of the injection process or to subpopulations of an inhomogeneous distribution of dye−semiconductor distances and couplings? Or does the main discrepancy in injection times found in various studies result from different experimental conditions, for example, sample preparation and data analysis. Our aim is to develop a dye−semiconductor system (employing TiO_2 thin film) where the electron transfer process can be clearly observed and thoroughly investigated. Having identified such a system, properties such as solvent, TiO_2 particle size, etc. can be modified such that the injection and recombination rates are optimized.

The xanthene dye Fluorescein 27 was found to be a suitable model compound for studies of electron injection and recombination. These processes have already been characterized for several xanthene dyes adsorbed at ZnO or TiO_2 electrodes or particles.[26−28] Recently, a femtosecond study on Fluorescein 27 adsorbed on TiO_2 colloidal particles in aqueous solution reported that electron injection occurs with a characteristic time constant of 300 fs.[20] In addition, a functional solar cell was constructed on the basis of polycrystalline TiO_2 layers sensitized with Fluorescein 27 and containing I^-/I_3^- ions in aqueous solution.[20]

In this paper, we report results of a detailed femtosecond transient absorption study focusing on porous TiO_2 film sensitized by the Fluorescein 27 dye and containing acetonitrile as solvent. As mentioned above, all previous studies of electron injection and recombination utilizing visible spectral region have suffered from the extensive spectral overlap of the transient signals of different electronic states. Our work shows that for the Fluorescein 27−TiO_2 film system there is also significant spectral overlap of the various transients, but by measuring transient spectra and kinetics over a wide spectral region (from 400 to 2000 nm), spectral windows can be identified where the decay of the reactant state (excited state of the dye) and the rise of the photoproducts (injected electrons and oxidized dye) can be recorded separately. To the best of our knowledge, this is the first reported study on a dye/TiO_2 film system in a solvent environment at normal laboratory conditions where the disappearance of the electron from the photoexcited dye and its appearance in the TiO_2 simultaneously can be followed in the visible spectral region on the femtosecond and picosecond time scales.

II. Experimental Section

1. Sample Preparation. The preparation method of the TiO_2 film is similar to that reported by other authors.[29] Briefly, to obtain a transparent TiO_2 thin film, a sol gel was prepared by dropping 10 ml of $TiCl_4$ (91 mM) at −20 °C slowly into 1 l of deionized water at 1 °C under vigorous stirring. After continuous stirring at this temperature, the reaction mixture was dialyzed against deionized water at room temperature until pH 3 and was concentrated by rotary evaporation at 30 °C to reach a TiO_2 concentration of up to 2 wt %. Finally, carbowax 2000 was added as a binder to increase the porosity of the final TiO_2 film, and the sol is ready to be spread on a substrate. For obtaining a film of uniform thickness of ~1 μm, we used scotch tape as framer and a glass rod to spread a drop of the viscous TiO_2 sol over a 0.6−0.8 × 76 × 26 mm microscope glass coverslip. The film was dried in air at room temperature for about 2 h and finally sintered at 350−400 °C for 1 h to obtain a perfectly transparent TiO_2 film consisting of relatively monodisperse particles of ~4 nm diameter, as determined by transmission electron microscopy (TEM). Their crystal structure has previously been determined to be that of anatase.[29] The thickness of the TiO_2 film was measured to be 1 ± 0.1 μm by both interference pattern in the VIS absorption spectrum and by a profilometer.

The Fluorescein 27 laser dye was used as purchased from Lambda Physik. Sensitization of the TiO_2 film was carried out by soaking the film in a 1.5×10^{-4} M solution of Fluorescein 27 in CH_3CN. The absorbance of the dye-sensitized films was kept at approximately 1.0−1.1 at 510 nm ($S_0 \rightarrow S_1$ absorption maximum). After the sensitization procedure the film was dried, then purged with CH_3CN and dried again, and finally covered with CH_3CN containing KI (0.1 M) and a thin 50 μm × 60 mm × 26 mm microscope glass coverslip. After the dye-sensitized film was purged with CH_3CN the optical density of the sensitized film did not change, showing that all dye molecules were adsorbed to the surface. KI was used to increase injection yield and stability of the samples. Measurements were performed on samples with and without KI.

For all measurements presented here the same TiO_2 film was used, to avoid the small variations in the dynamics for different films. Nonetheless, very similar dynamics were observed in other films, prepared according to the same procedures. Recycling of the film between measurements consisted in

washing out the dye with NaOH and deionized water and heating to 150 °C. To prevent degradation of the adsorbed dye due to laser light irradiation, the sample was continuously moved during measurements by using a X−Y translation stage.

2. Femtosecond Spectrometer. Femtosecond measurements were performed on a differential absorption spectrometer based on a regeneratively amplified mode-locked 5 kHz repetition rate Ti:sapphire laser system in combination with an optical parametric amplifier (OPA).[30] To resolve the initial dynamics following photoexcitation of the adsorbed dye, we have used femtosecond pump−probe spectroscopy, exciting the dye with a 510 nm, ∼100 fs laser pulse. A typical excitation pulse energy of ∼0.5 μJ was used with a spot size diameter of ∼400 μm at the sample position. For the generation of probe and reference light, part of the amplified fundamental laser beam was sent into either a quartz or sapphire plate to generate a white-light continuum. In the region from 1200 to 2000 nm another OPA was used to generate the probe light. The polarization of the analyzing beam was fixed via a Glan polarizer, while a Berek compensator was used to rotate the polarization of the excitation beam to parallel orientation. For selecting the detection wavelength, the probe and reference beams were dispersed in a monochromator. The spectral resolution of the detection system was 5 nm. The transient absorption signal was measured by detecting the probe, reference, and part of the excitation light with three photodiodes in a single shot detection system. Changes in absorbance as low as 10^{-5} could be recorded by this system. The instrument response function of 130−200 fs (fwhm) depending on wavelength (400−2000 nm) was determined by sum frequency cross correlation in a BBO crystal. For monitoring the transient absorption dynamics two different measurements were performed: (1) at a fixed detection wavelength transient absorption kinetics were recorded by scanning the pump−probe delay time; (2) at a fixed pump−probe delay time transient absorption spectra were recorded by scanning the detection monochromator in the 400−2000 nm spectral region. Compensation for group velocity dispersion was performed by properly shifting the delay line to keep the pump−probe delay fixed for each wavelength. The accurate zero-time delay at all measured wavelengths was independently determined by sum frequency cross-correlation measurements and by the nonresonant "spike-signal" in a water cell and in a 1 mm thick glass plate. For very precise determination of the zero-time, the low amplitude "spike signal" ($\Delta A_{max} < 1.0 \times 10^{-4}$; Figure 4 inset) generated in a 50 μm glass slide was recorded (such a thin glass slide was used as front window of our sample cell). All experiments were conducted at room temperature.

Measured kinetics were analyzed with the deconvolution software Spectra Solve 2.01, LASTEK Pty. Ltd. 1997. Global analysis of spectral data recorded from 400 to 600 nm was performed by applying the principal component analysis (PCA) method, using Matlab software (1992). Detailed presentation of the analysis will be published elsewhere.[31]

III. Results and Discussion

The steady-state absorption spectrum of the Fluorescein-sensitized TiO_2 thin film is shown in Figure 1 (bold dashed line). The chemisorption of the dye, presumably via the carboxylic group to the TiO_2 film, is assumed to be very strong since the optical density does not decrease upon leaving the sensitized film in pure acetonitrile overnight. The good stability of the adsorbed dye was confirmed by kinetic measurements at various excitation intensities, showing linear intensity dependence of the signal amplitude. The extinction coefficient of

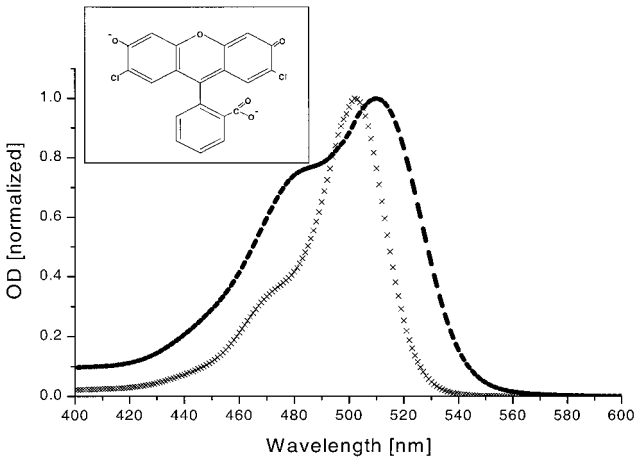

Figure 1. Normalized steady-state absorption spectra: Fluorescein 27 adsorbed to TiO_2 film covered with CH_3CN (dashed bold line); Fluorescein 27 in aqueous pH > 10 solution (crosses). Inset: structure of Fluorescein 27, dianionic form. The adsorption of the dye to the TiO_2 occurs presumably via the carboxylic group.

adsorbed dye was determined by the following procedure. Practically all the dye molecules can be desorbed from the TiO_2 film into pH = 11 H_2O. Knowing the extinction coefficient of the dye in aqueous solution at pH > 10 to be $\epsilon = 6.5 \times 10^4$ M^{-1} cm^{-1} the overall number of desorbed dye molecules can be calculated, giving the dye concentration in the particular volume of the film. From the optical density of the sample we calculate the extinction coefficient of the surface adsorbed dye to be $\epsilon = 3.1 \times 10^4$ M^{-1} cm^{-1}, which yields an optical cross section of 1.2×10^{-16} cm^{-2}. The shape of the steady-state spectrum does not depend on the adsorbed dye concentration. To determine the number of TiO_2 particles that constitute the particular film, the following parameters were taken from the TEM picture: size of the particle (3.5 ± 1 nm) and the ∼50% porosity of the film. In our films of bypiramidal morphology TiO_2 nanoparticles, 5−6 dye molecules on average are adsorbed to every particle.

For measurements on the nonadsorbed dye, 0.8 μM Fluorescein in aqueous solution at pH >10 (dianionic form) was used (absorption spectrum shown with crosses in Figure 1). The protonation state of both surface bound dye and of the dye in pH >10 solution is the same; the spectra are spectroscopically similar and the extinction coefficients are comparable.

Figure 2 shows the transient absorption spectrum of the Fluorescein 27-sensitized TiO_2 film (filled squares) measured at 500 fs after 510 nm laser excitation. The early photoinduced absorption dynamics of the sensitized film exhibit negative signals from ground-state bleaching and SE in the spectral region of the steady-state absorption and fluorescence of the system (from 460 nm to ca. 650 nm), as well as positive signals (ESA and products) from 400 to 460 nm and between 670 and 2000 nm. To quantify the time evolution of the observed spectral features in the spectral region of ground-state bleach and SE, kinetics were measured at several different wavelengths between 470 and 650 nm. We conclude that the kinetics measured in the wavelength region 560−600 nm reflect the decay of SE since ground-state bleaching can be ignored in this wavelength interval (see absorption spectrum in Figure 1) and the SE decay at all wavelengths can be characterized with the same kinetics. In other words, were there substantial contributions to the transient spectrum from other processes, e.g., ground-state bleach recovery or photoproduct formation and decay, we would expect to see kinetic components characteristic of these reactions

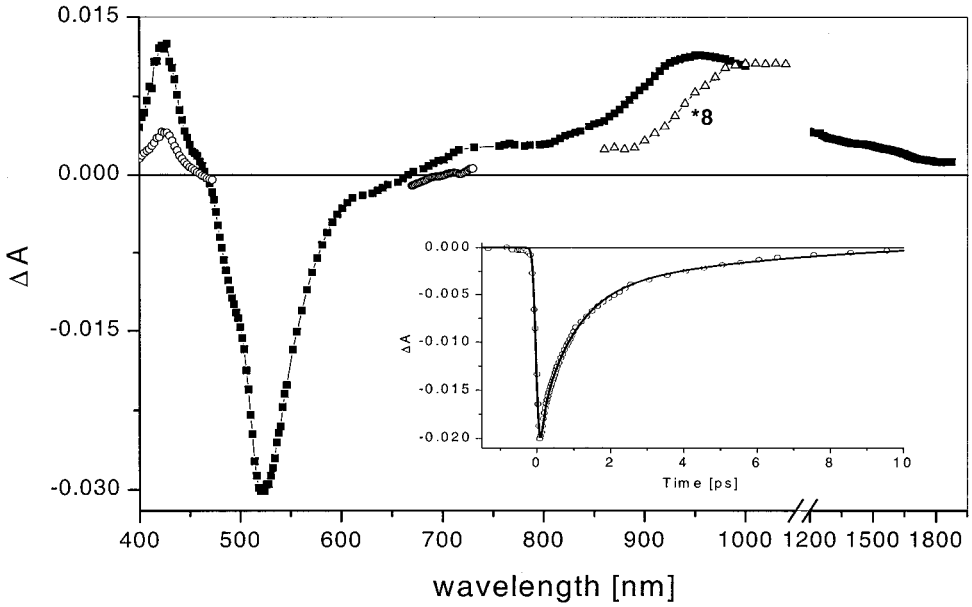

Figure 2. Transient visible and near-IR absorption spectra measured 500 fs after laser excitation at 510 nm: Fluorescein 27-sensitized TiO_2 film covered with CH_3CN in the presence of KI (filled squares); Fluorescein 27 in aqueous pH > 10 solution (open circles); Fluorescein 27 in aqueous pH > 10 solution scaled to the spectrum of sensitized film (open triangles, scaled by a factor of 8 to match the signal from the film). Concentrations and optical path as indicated in the text. For measurements on the dye in solution the polarization angle between pump and probe beams was set to the magic angle 54.7°. Inset: transient absorption kinetics of stimulated emission decay at 580 nm. Circles are measured data, curve is fit with the following time constants and initial amplitudes (in parentheses): 0.08 ps (31%), 0.9 ps (50%), 7 ps (20%), and >1 ns (−1%).

(much more long lived, see below). The SE kinetics are highly nonexponential and show that the fluorescence of the Fluorescein-sensitized TiO_2 film is quenched within a few picoseconds, although the dye in solution exhibits a long-lived excited state (nanosecond time scale). The excitation intensity of $\sim 10^{14}$ photons pulse^{-1} cm^{-2} (0.5 μJ/pulse) used in the experiments was far from the saturation limit considering the optical cross section of the adsorbed dye to be 1.2×10^{-16} cm^{-2}. Indeed, no dependence on excitation intensity of the kinetics at 535 nm (bleach and SE) was observed when the energy of excitation was varied from 0.2 to 0.8 μJ/pulse (data not shown). The inset of Figure 2 represents one example of the SE decay at 580 nm. The best fit to the signal yields a multiexponential decay with the following time constants and initial amplitudes (in parentheses): 0.08 ps (31%), 0.9 ps (50%), 7 ps (20%), and >1 ns (−1%). Since a solar cell based on Fluorescein 27 sensitized TiO_2 was shown to work,[20] it is reasonable to assume that the fluorescence of the system is quenched by the electron injection from the excited state of the dye molecule to the semiconductor and that the time constants of SE decay characterize the electron injection lifetimes.

To examine the corresponding formation of the photoproducts, conduction band electrons and oxidized dye molecules (D^+), kinetics were recorded throughout the positive transient absorption spectrum of Fluorescein-sensitized TiO_2 film. Kinetics measured at three wavelengths (440, 960, 1530 nm) are shown in Figure 3 along with the SE decay at 580 nm. For a critical comparison of the kinetics, the traces are vertically translated to a common short time (4−5 ps) level and normalized to unity at the maximum. Within experimental error all kinetic traces have the same temporal evolution on the few picosecond time scale. The fits to the kinetics in Figure 3 yield instrument response limited rise times and multiexponential decay functions; very similar kinetics are observed at other wavelengths, between 400 and 2000 nm. We note that kinetics measured between 400 and 450 nm are distorted at $t \approx 1.5$ ps, presumably

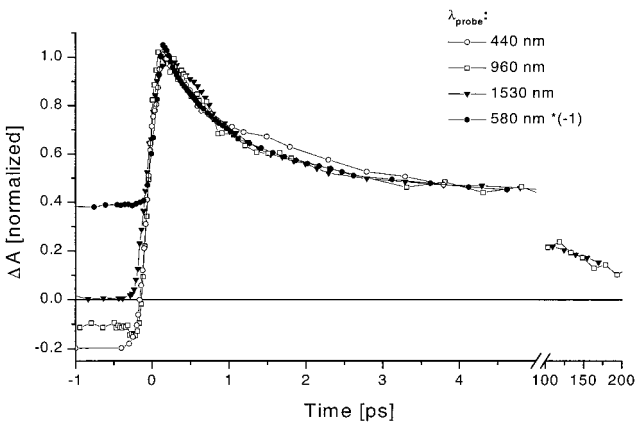

Figure 3. Comparison of transient absorption kinetics at different wavelengths. The traces are vertically translated to a common short time (4−5 ps) and normalized to unity at the maximum.

because of overlap between different signal contributions from various electronic states of the dye and the oxidized dye.

This similarity of SE and induced absorption decay kinetics on a short time scale, and the fact that no rise component was resolved for the positive signals at most wavelengths, could imply that either the electron injection is faster than we can resolve or the induced absorption ESA is overwhelming the photoproduct absorption. However, by performing a careful analysis of photoinduced dynamics in the two spectral regions where the transient spectrum of the dye in aqueous solution changes sign, i.e., around the $\Delta A = 0$ crossing points at 460 nm and at 700 nm (see Figure 2), we can resolve the kinetics of product formation (electron injection) free of influence from ESA. The importance of these spectral regions and how they can be exploited to provide information on the electron injection process is discussed below. In the case of the dye in solution both crossing points are isosbestic points (time independent $\Delta A = 0$ crossing points). At both wavelengths the signals are related

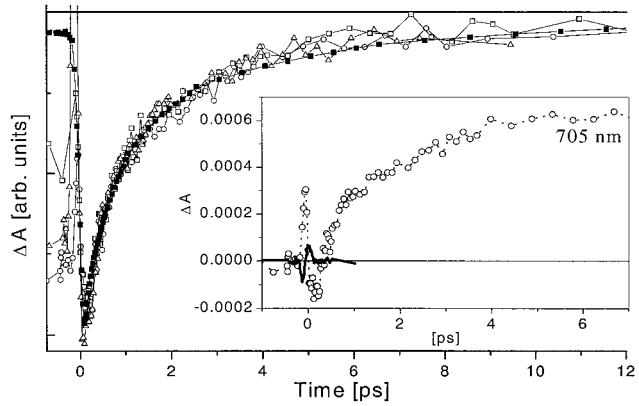

Figure 4. Comparison between transient absorption kinetics of SE decay at 580 nm (filled squares) and of induced rise kinetics of conduction band electrons measured around the $\Delta A = 0$ crossing point (~700 nm), 690 nm (open squares), 695 nm (open triangles), 705 nm (open circles). In the inset, the kinetics recorded at 705 nm is presented (open circles) together with the low amplitude spikelike signal induced in the 50 μm thick front window of our sample (solid line).

to the same process of deactivation of the excited-state population back to the ground state. Particularly at 700 nm, the signals that cancel each other (ESA and SE) both belong to the same transient species, excited-state population. According to these considerations, in the dye-sensitized TiO_2 film the crossing point at ~700 nm would be an isosbestic point as long as no other species contributes to the signal. If for instance, a photoproduct would be formed from the excited state of the dye molecule and absorbs in this wavelength region, we would be able to detect its formation at this isosbestic point of the dye in solution, even if the absorbance of the product is much smaller than the signal amplitude of SE and ESA at other wavelengths. In the experiment this would be resolved as a time dependent shift in the wavelength of the crossing point. Thus, if only the dye excited state is present at early times, the $\Delta A = 0$ crossing point is expected to be close to the wavelength observed in solution, but it would evolve toward other wavelengths at later times with the buildup of products.

We now examine how the $\Delta A = 0$ crossing point at ~700 nm can provide information about the electron injection process. Tuning the probe light of our femtosecond spectrometer in the spectral region around 700 nm, induced absorption kinetics with pronounced rise times were observed. The inset of Figure 4 shows the low amplitude transient kinetics measured for a Fluorescein-sensitized TiO_2 film at 705 nm (open circles). The main panel of Figure 4 shows kinetics with induced rise times at 690, 695, 705 nm and the decay of SE at 580 nm; the rise of the signals measured close to the isosbestic point of the dye in solution matches the decay times of the SE. The extinction coefficient of the absorbing species we estimated to be ~3000 M^{-1} cm^{-1} at 700 nm from the ratio of transient absorption signals at 510 nm (absorption maximum) and 700 nm, using the extinction coefficient of the adsorbed Fluorescein 27 dye and the value of Stokes shift between the linear absorption and its emission mirror image of the Fluorescein-sensitized TiO_2 film, calculated from the measured differential spectra. This value of the extinction coefficient at 700 nm coincides perfectly with the extinction coefficient of conduction band electrons in TiO_2 particles (~3000 M^{-1} cm^{-1} at 700 nm).[32,33] It should also be emphasized that the measured signals are free of artifacts resulting from impulsive stimulated Raman, cross phase modulation, etc. from the front window of the sample and/or solvent. The spikelike signal induced in the very thin (50 μm) first

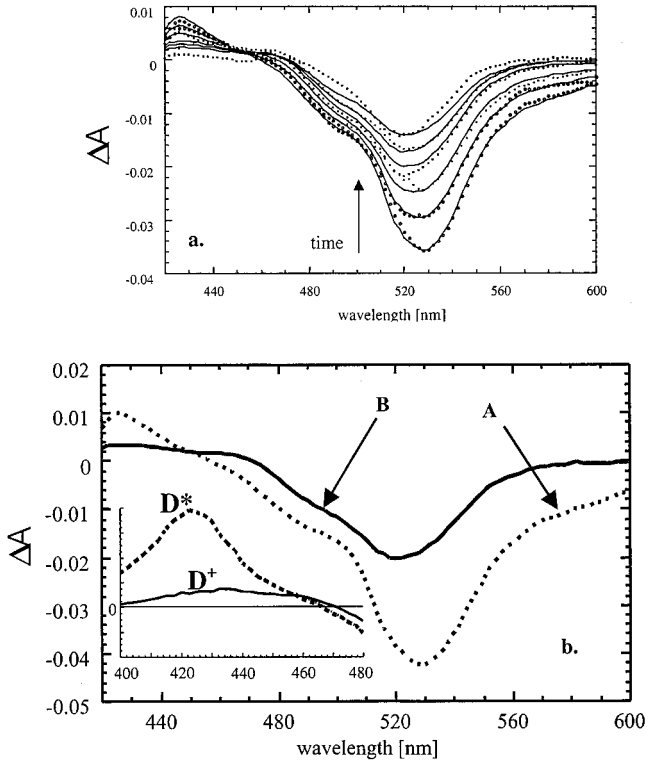

Figure 5. (a) Transient absorption spectrum of Fluorescein 27-sensitized TiO_2 film with KI in CH_3CN, in the wavelength region 400−600 nm, at delay times from 1.3 to 40 ps (the arrow indicates the time evolution): dots, experimental points; solid lines, kinetic fit with double-exponential function. For these measurements excitation pulses of higher intensities (~0.75 μJ) were used. (b) Calculated species associated spectra from Figure 5a: component A is assigned to the mixture of ESA, SE, and ground-state bleach; component B is assigned to absorption of oxidized dye and ground-state bleach. Inset: species-associated spectra only from 400 to 480 nm; component D* is associated with a hot excited state that due to electron injection decays to component D^+, assigned to absorption of oxidized dye.

window of our sample is shown in the inset of Figure 4, as a solid line. The thick (~1 mm) back window (substrate) does not contribute much to the spikelike signal, since the optical density of the sample allows only a small portion of excitation light to reach the back window. The solvent contribution to the signal is negligible, since the thickness of the solvent is of the order of the thickness of the film (~1 μm). Hence, the fast process at the beginning of the trace ($t \approx 0$) is characteristic of the Fluorescein 27 dye and as confirmed by measurements on both dye in solution and the dye-sensitized film, no induced rise of the signal is accompanying this fast process; it appears only as an oscillatory signal, which is over in ~200 fs.

In the case of the dye-sensitized film, at the crossing point at ~460 nm both the ground state and the excited state contribute to the signal. If electron injection occurs from the excited state of the dye into TiO_2, the dye molecule does not return to the ground state and there is consequently no recovery of ground-state bleaching. Therefore, the crossing point at 460 nm should blue shift as the ESA decays due to decay of the excited-state population. Contrary to this expectation, we observe a red shift of the spectrum with time, presumably caused by induced absorption of a product. Global analysis of spectral data recorded from 400 to 600 nm at delay times from 1.3 to 40 ps (Figure 5a) reveals a buildup of a product state with broad, unstructured absorption around 430−450 nm, the spectral region where the chemically oxidized Fluorescein dye is known to absorb light.[34,35] The formation of this product (presumably the oxidized

dye molecule) on the time scale >1 ps is characterized by a 3 ps time constant (from the global fit), very similar to the slower parts of the SE decay. There are also faster components of this buildup, but as mentioned above the interference between ESA and product formation in the 400−450 nm spectral region makes it difficult to accurately characterize this part of the spectral dynamics. Kinetics with similar rise times to the kinetics measured at around 700 nm were recorded at 465 nm (data not shown).

1. Electron Injection. As discussed above, the precursor and the product states of electron injection do not have clearly different spectra in the VIS and NIR. Regions where the different species can be distinguished is the region of SE decay and around the $\Delta A = 0$ crossing points. While the decay of SE can be detected over a wide probing wavelength interval (between 560 and 600 nm) and gives very strong transient signal that is dominant over the absorption of other species, the formation of photoproducts can be recorded only in spectral regions where the net transient absorption is given by the overlap of various signals. To bypass this complexity, we are measuring the formation of photoproducts in well-defined spectral windows (700 ± 10 and 460 ± 5 nm) where two signals out of the three that are contributing to the net signal cancel each other and the remaining one reflects the photoproduct dynamics.

The systematic study performed around the isosbestic points of the dye in solution and the good agreement between the decay of SE and the induced rise of photoproducts unambiguously show that SE decays because electrons are injected into the TiO_2 semiconductor from the photoexcited Fluorescein 27 dye. The induced absorption kinetics recorded around the crossing point at 700 nm, showing the appearance (and disappearance) of a photoproduct, we attribute mainly to conduction band electrons.

In addition to the absorption of conduction band electrons and SE decay, the dynamics of D^+ can also be used for monitoring electron injection in sensitized semiconductor systems. We mentioned above that a global analysis of the spectral evolution in the 400−600 nm spectral region yields a ~3 ps time constant for the formation of oxidized dye upon electron injection. In Figure 5b we show the results of this analysis as the species associated spectra of our reaction model. Briefly, the dotted line represents component A that can be assigned to the mixture of ESA, SE, and ground-state bleach, and which decays to D^+ and ground-state bleach, component B (solid line). The transformation of the molecule and formation of D^+ in the course of electron injection is clearly illustrated by the spectral dynamics in the 400−480 nm region (see inset of Figure 5b), as the $D^* \rightarrow D^+$ process. The oxidized dye state decays on a longer time scale (from approximately a few tens of picoseconds to longer times) to the ground state of the dye, due to reduction by I^- or recombination with injected electrons. A detailed kinetic study of this spectral region will be presented elsewhere.[31]

Finally, we discuss the origin of the induced absorption in the near-IR parts of the transient absorption spectrum (>800 nm). Relatively strong ESA of the Fluorescein 27−TiO_2 system appears instantaneously in the spectral region where the ESA of the dye in aqueous solution is weak (850−1050 nm) or too low to be detected (1200−2000 nm), although the extinction coefficient of the ground-state absorption of the dye adsorbed to the TiO_2 is smaller than the extinction coefficient of the dye in aqueous solution. According to our findings, using the dye in solution to exclude ESA in a particular spectral region (near-IR) and thereby attributing transient absorption signals to the dynamics of photoproducts is not a very reliable approach. Interaction between the dye and the semiconductor due to adsorption and binding severely affects ESA. In our system, electron injection can be monitored in the visible spectral region by probing the absorption of conduction-band electrons in TiO_2 and/or oxidized dye in specific wavelength regions. The dynamics of electron injection is multiexponential, characterized by the following time constants: <0.1, 0.9 ± 0.2, and 8.0 ± 2.0 ps.

Our results on electron injection show remarkable agreement with a recent study of electron injection from ruthenium bipyridyl and porphyrin sensitizer dyes to TiO_2 film, reported by Klug et al.[19] The good agreement of injection dynamics for several different dyes (ruthenium dyes, porphyrins, and now a xanthene dye) with very different photophysical properties supports the suggestion by Klug et al.[19] that the characteristics of interfacial electron injection are not determined by the properties of the sensitizing dye, but rather by the linkage of the dye to the TiO_2 film. For the dyes studied by Klug et al., as well as in the present molecule, the adsorption to the TiO_2 surface is achieved by carboxylate group(s). For all molecules, the kinetics of electron injection are multiexponential, requiring a minimum of three time constants ranging from <100 fs to ~10 ps. The multiexponential nature of electron injection is probably associated with the heterogeneity of the semiconductor. By performing precise transient absorption measurements over a broad spectral region and carefully accounting for the dye ESA signals, we have succeeded to observe the formation of conduction band electrons in the visible/near-IR spectral region and to correlate their formation kinetics to the decay of the system SE and appearance of the oxidized dye molecule. The comparison between injection times for samples with and without KI shows no major difference. Within our accuracy, the presence of I^- does not influence the injection dynamics. The effect of K^+ is not evident since due to recycling of the TiO_2 films our sample contains Na^+, which is known to give a higher injection quantum yield than K^+.[36] Without a detailed study, no clear conclusions can be drawn about the effect of cation-controlled injection[36] on the femtosecond time scale.

Electron Recombination. Above we have shown how SE decay, formation of oxidized dye, and appearance of conduction band electrons monitor the electron injection. Similarly, the decay of conduction band electrons, decay of oxidized dye, and ground-state recovery (GSR) can be used to characterize the recombination process. Our earlier studies of electron injection and recombination in Fluorescein 27-sensitized TiO_2 colloidal particles,[20] indicated that recombination may be controlled by a solvation process or by a conformational change of the dye molecule. In an operating solar cell, a high concentration of I^- ions are present that may influence the recombination processes. We have measured the recombination for Fluorescein 27-sensitized TiO_2 films with and without KI added to the solvent. The recombination was monitored by the conduction band electron signal around 700 nm. Kinetics measured at 705 (Figure 6, closed circles) for the KI-free sample suggest a widely distributed recombination rate, ranging from a few tens of picoseconds up to longer times. The observed fast partial decay of the signal is characterized by $\tau_{1/2} \sim 40$ ps. The signal reaches a constant level at ~80 ps. The kinetics indicate that the majority of the electrons do not recombine on the investigated time scale (until 500 ps). The nonexponential nature of the electron recombination, with kinetic components ranging from tens of picoseconds to longer times has been noticed in previous works.[8−25] This behavior was mainly attributed to both spatial and energetic distribution of the trapped electrons in the

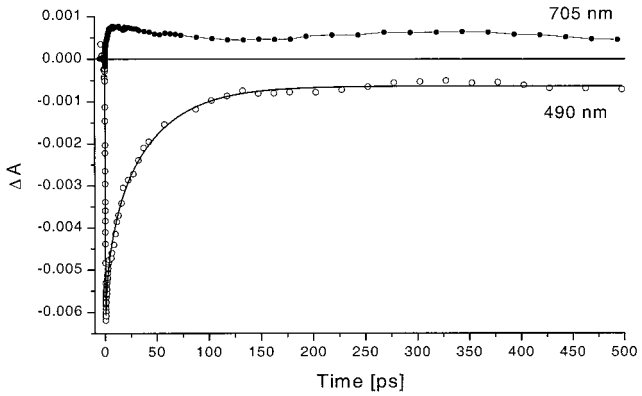

Figure 6. Long-time comparison of conduction band electron signal measured at 705 nm (filled circles) and kinetics measured at 490 nm (open circles) for KI free Fluorescein-sensitized TiO_2 film with CH_3-CN as solvent. Solid line, fit with the following time constants and initial amplitudes (in parentheses): 1 ps (~10%), 8 ps (~20%), 40 ps (~60%), and >1 ns (~10%).

semiconductor. We do not examine these issues further here. A weak oscillatory modulation of the recombination signal is observed on the >100 ps time scale (see Figure 6). This feature will be discussed in more detail elsewhere.[31]

The signal at ~490 nm also contains information about the electron recombination process (through the oxidized dye molecule), but the transient absorption at this wavelength is complex as it has contributions from dye ESA, absorption of D^+, and ground-state bleaching. The decay at 490 nm (Figure 6, open circles) is nevertheless very informative from the point of view that it reflects the whole charge-transfer process. Knowing the injection lifetimes from the SE and conduction band electron dynamics, we can assign the initial fast part of the decay at 490 nm (~1 ps (~10%) and ~8 ps (~20%) decay components) to the formation of D^+ and the later part (~40 ps (~60%) and >1 ns (~10%) decay components) to the decay of D^+ and recovery of the ground state by electron recombination. The ~40 ps and >1 ns decay components agree very well with the recombination kinetics measured at 705, again showing that electron$-D^+$ recombination is a nonexponential process and that a major part of the oxidized dye molecules and electrons persist for a time much longer than 500 ps. It is important to point out that the amplitude (~10%) of the nondecaying component of the signal measured at 490 nm does not provide direct information on the fraction of reduced D^+, due to the compound nature of the transient absorption signal at this wavelength. This information is obtained from the signal measured at ~700 nm, which directly probes the concentration of injected electrons.

When KI is added to the sample, D^+ can be reduced by I^- ions and/or can recombine with the injected electron. For the ruthenium sensitizing dyes, the latter process was shown to be slower than the reduction by ions.[7,37−39] Recently, Moser et al.[39] have examined with nanosecond resolution (flash photolysis) reduction of the $Ru^{II}(dcbpy)_2(NCS)_2$ cation by iodide on TiO_2 film by measuring recovery of bleaching signals of the dye/TiO_2 system with and without different cations in the electrolyte, and obtained sub-microsecond time constants for the half-lifetime of the dye ground-state regeneration. Comparing bleach signals in the Fluorescein 27$-TiO_2$ system we found that the decay of the oxidized dye is faster in the sample that contains KI compared to the KI-free sample. The half-lifetime of the fast initial recombination decay component at 490 nm is ~25 ps (data not shown), while in the absence of KI it is ~40 ps. These results suggest that the fast part of the D^+ decay is accelerated by the addition of I^- and that reduction of D^+ by I^- ocurs on the ~70 ps time scale. The origin of this fast D^+-I^- reduction is probably because of direct contact between a fraction of iodide atoms and dye molecules, similar to what has already been suggested in previous works.[39,40] The initial oxidation of I^- to the thermodynamically unfavorable iodine atom is followed by the reaction with a free I^- to form $I_2^{\bullet-}$.[41] The extinction coefficient of $I_2^{\bullet-}$ [40,42] would allow its detection with our spectrometer, but a significant amount of $I_2^{\bullet-}$ was not observed on the time scale of our measurements (up to 500 ps) because of the slow diffusion-controlled formation of $I_2^{\bullet-}$.

Conclusions. We have shown that electron injection from the photoexcited Fluorescein 27 dye molecules into a TiO_2 nanostructured film occurs on the femtosecond and picosecond time scales, by clearly resolving the dynamics of conduction band electrons and oxidized dye molecules in the visible spectral region around the isosbestic points of the dye in solution. It was demonstrated that SE decay is caused by the charge injection and that the decay of SE is directly correlated to the formation of conduction-band electrons and oxidized dye molecules. Moreover, the measurements provide evidence that relatively strong ESA of the dye$-TiO_2$ system appears instantaneously in the spectral region where neither the TiO_2 nor the dye in solution has any absorption, suggesting that the interaction between the dye and the semiconductor due to adsorption and binding severely affects the ESA.

Nonetheless, by carefully choosing spectral regions where the ESA of the dye/semiconductor is canceled, the electron injection and recombination can be studied in detail. The Fluorescein 27$-TiO_2$ system holds good promise to be a tool for developing a more detailed description of electron transfer in nanostructured dye-sensitized TiO_2 films.

Acknowledgment. This work was funded by grants from the Delegationen for Energiförsörjning i Sydsverige (DESS), the Knut and Alice Wallenberg Foundation, the Crafoord Foundation and the Trygger Foundation. M.H. acknowledges receipt of a travel grant from the European Union (Contract ERBFMGECT950020(DG12)). We thank Dr. A. Hagfeldt for helpful discussions and Dr. J. L. Herek for critical reading of the manuscript.

References and Notes

(1) Tani, T. *J. Imaging Sci.* **1990**, *34*, 143−148.
(2) Tani, T.; Suzumoto, T.; Ohzeki, K. *J. Phys. Chem.* **1990**, *94*, 1298−1301.
(3) Kiess, H. *Prog. Surf. Sci.* **1997**, *9*, 113−142.
(4) Hammarström, L.; Sun, L.; Åkermark, B.; Styring, S. *Biochim. Biophys. Acta* **1998**, *1365*, 193−199.
(5) Bolton, J. R. *Solar Energy Mater. Solar Cells* **1995**, *38*, 543−554.
(6) Schmelling, D. C.; Gray, K. A.; Kamat, P. V. *Environ. Sci. Technol.* **1996**, *30*, 2547.
(7) Hagfeldt, A.; Grätzel, M. *Chem. Rev.* **1995**, *95*, 49−68.
(8) Nazeeruddin, M. K.; Kay, A.; Rodicio, I.; Humphry-Baker, R.; Muller, E.; Liska, P.; Vlachopoulos, N.; Grätzel, M. *J. Am. Chem. Soc.* **1993**, *115*, 6382−6390.
(9) O'Regan, B.; Grätzel, M. *Nature* **1991**, *353*, 737−739.
(10) Burfeindt, B.; Hannappel, T.; Storck, W.; Willig, F. *J. Phys. Chem.* **1996**, *100*, 16463−16465.
(11) Hannappel, T.; Burfeindt, B.; Storck, W.; Willig, F. *J. Phys. Chem. B* **1997**, *101*, 6799−6802.
(12) Hannappel, T.; Zimmermann, C.; Meissner, B.; Burfeindt, B.; Storck, W.; Willig, F. *J. Phys. Chem. B* **1998**, *102*, 3651−3652.
(13) Ellingson, R.; J.; Asbury, J.; B.; Ferrere, S.; Ghosh, H. N.; Sprague, J.; Lian, T.; Nozik, A. J. *J. Phys. Chem. B* **1998**, *102*, 6455−6458.
(14) Ghosh, H. N.; Asbury, J.; B.; Lian, T. *J. Phys. Chem. B* **1998**, *102*, 6482−6486.
(15) Asbury, J.; B.; Ellingson, R.; Ghosh, H.; J.; Ferrere, S.; N.; Nozik, A. J.; Lian, T. *J. Phys. Chem. B* **1999**, *103*, 3110−3119.

(16) Ghosh, H. N.; Asbury, J.; B.; Weng, Y.; Lian, T. *J. Phys. Chem. B* **1998**, *102*, 10208−10215.
(17) Tachibana, Y.; Moser, J. E.; Grätzel, M.; Klug, D. R.; Durrant, J. R. *J. Phys. Chem. B* **1996**, *100*, 20056−20062.
(18) Moser, J. E.; Dimitrios, N.; Bach, U.; Tachibana, Y.; Klug, D. R.; Durrant, J. R.; Robin. H.-B.; Grätzel, M. *J. Phys. Chem. B* **1998**, *102*, 3649−3650.
(19) Tachibana, Y.; Haque, S. A.; Mercer, I. P.; Durrant, J. R.; Klug, D. R. *J. Phys. Chem. B* **2000**, *104*, 1198−1205.
(20) (a) Hilgendorff, M.; Sundström, V. *J. Phys. Chem. B* **1998**, *102*, 10505−10514. (b) Hilgendorff, M.; Sundström, V. *Chem. Phys. Lett.* **1998**, *287*, 709−713.
(21) Martini, I.; Hodak, J. H.; Hartland, G. V. *J. Phys. Chem. B* **1998**, *102*, 9508−9517.
(22) Martini, I.; Hodak, J. H.; Hartland, G. V. *J. Phys. Chem. B* **1999**, *103*, 9104−9111.
(23) Huang, S. Y.; Schlichtrorl, G.; Nozik, A. J.; Grätzel, M.; Frank, A J. *J. Phys. Chem. B* **1997**, *101*, 2576−2582.
(24) Ghosh, H. N. *J. Phys. Chem. B* **1999**, *103*, 10382−10387.
(25) Weng, Y.-Q.; Wang, Y.-X.; Asbury, J.; B.; Ghosh, H. N.; Lian, T. *J. Phys. Chem. B* **2000**, *104*, 93−104.
(26) Memming, R. *Photochem. Photobiol.* **1972**, *16*, 325.
(27) Gerischer, H.; Willig, F. *Topic. Curr. Chem.* **1976**, *61*, 33.
(28) Moser, J. E.; Grätzel, M.; Sharma, D. K.; Serpone, N. *Helv. Chim. Acta* **1985**, *68*, 1686.
(29) (a) Kalyanasundaram, K.; Grätzel, M. *Proc. Indian Acad. Sci. (Chem. Sci.)* **1997**, *109*, 447−49. (b) The crystal structure was determined by XRD analysis and electron diffraction measurements by M. Hilgendorff et al., Hahn-Meitner Institute, Berlin (not published result).
(30) Chachisvilis, M.; Kühn, O.; Pullerits, T.; Sundström, V. *J. Phys. Chem. B* **1997**, *101*, 7275.
(31) Benkö, G.; Yartsev, A.; Hilgendorff, M.; Sundström, V. Manuscript in preparation.
(32) Rothenberger, G.; Fitzmaurice, D.; Grätzel, M. *J. Phys. Chem.* **1992**, *96*, 5983−5986.
(33) Saleh, B. E. A.; Teich, M. C. *Fundamentals of Photonics*; John Wiley & Sons, Inc.: New York, 1991.
(34) Linquist, L. *Ark. Kemi* **1960**, *16*, 79−140.
(35) Cordier, P.; Grossweiner, L. L. *J. Phys. Chem. B* **1968**, *72*, 2018−2024.
(36) Kelly, A. C.; Farzad, F.; Thompson, D. W.; Stipkala, J. M.; Meyer, G. J. *Langmuir* **1999**, *15*, 7047−7054.
(37) Huang, S. Y.; Schlichthörl, G.; Nozik, A. J.; Grätzel, M.; Frank, A. J. *J. Phys. Chem. B* **1997**, *101*, 2576−2582.
(38) Haque, S. A.; Tachibana, Y.; Willis, R.; Moser, J. E.; Grätzel, M.; Klug, D. R.; Durrant, J. R. *J. Phys. Chem. B* **2000**, *104*, 538−547.
(39) Pelet, S.; Moser, J. E.; Grätzel, M. *J. Phys. Chem. B* **2000**, *104*, 1791−1795.
(40) Fitzmaurice, D. J.; Frei, H. *Langmuir* **1991**, *7*, 1129−1137.
(41) Fisher, A. C.; Peter, L. M.; Ponomarev, E. A.; Walker, A. B.; Wijayantha, K. G. U. *J. Phys. Chem. B* **2000**, *104*, 949−958.
(42) Baxendale, J. H.; Sharpe, P.; Ward, M. D. *Int. J. Radiat. Phys. Chem.* **1975**, *7*, 587−588.